Quantum State Filtering of Dual-rail Photons with Fiberized Plasmonic Metamaterial

Salih Yanikgonul[1,2,*], Anton. N. Vetlugin[1], Ruixiang Guo[1], Angelos Xomalis[3], Giorgio Adamo[1], Cesare Soci[1] and Nikolay I. Zheludev[1,3]

[1]*Centre for Disruptive Photonic Technologies, Nanyang Technological University, 637371, Singapore*
[2]*Institute of Materials Research and Engineering, Agency for Science, Technology and Research, 138634, Singapore*
[3]*Optoelectronics Research Centre & Centre for Photonic Metamaterials, University of Southampton, Southampton SO17 1BJ, UK*
**salih001@ntu.edu.sg*

Abstract:
We demonstrate quantum state filtering of dual-rail photons through single-photon interference on a fiberized plasmonic metamaterial, exploiting different optical response of the metamaterial to symmetric and anti-symmetric superpositions of double-path wavefunction of single-photons.

OCIS codes: 160.3918, 250.5403, 270.0270.

1. Introduction

Coherent interaction of light with nanostructured materials provides new possibilities for manipulation of photons in quantum communication systems [1, 2]. In this process, the interaction of two coherent beams of light on a layer of a plasmonic metamaterial is exploited so that one beam modulates the intensity of the other. Here we demonstrate that such subwavelength thick plasmonic metamaterials can also be used to modify wavefunctions of single photons. We demonstrate quantum state filtering of dual-rail photons in a stabilized fiber network by using a metamatarial, which has different optical responses to symmetric and anti-symmetric superpositions of double-path wavefunction of single-photons.

2. Experimental Setup

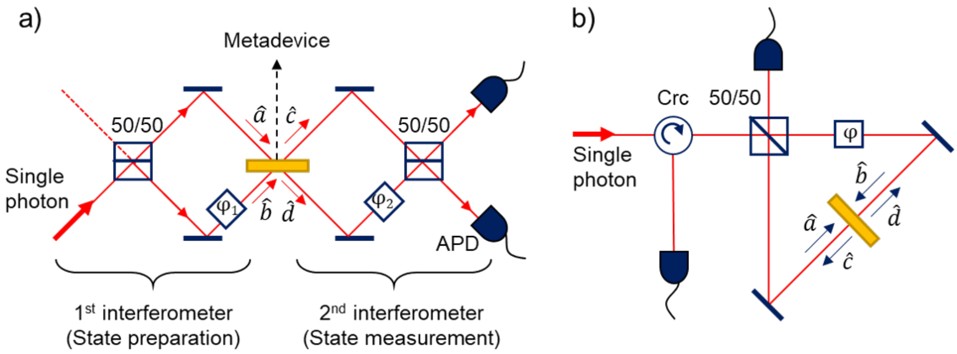

FIGURE 1: (a) The schematic of the double interferometer (ϕ_i, phase modulator; APD, single-photon avalanche diode; 50/50, 50/50 beam splitter), (b) the simplified schematic of the experimental setup we used to implement the double interferometer (Crc, optical circulator). Our metadevice consists of a subwavelength thick gold nanofilm engraved on an end facet of a single-mode fiber.

In our experiments, we adopted a double interferometer design as shown in Fig. 1(a), where one interferometer is used to prepare dual-rail superposition input states of single photons and the other one is used to perform projective measurements on photon output states. In the first interferometer, the phase retardation between two arms is controlled via a phase modulator ϕ_1. After a single-photon interacts with the metadevice, the state measurement on the output state is performed through single-photon interference in the second interferometer, where phase delay between interfering arms is controlled via ϕ_2. We implement this double interferometer design in a more compact way as shown in Fig. 1(b). In our setup, an incoming photon to the metadevice will traverse the first interferometric path, whereas the outgoing photon from the metadevice will traverse the second interferometric path and eventually be detected by single-photon detectors at the output port. The phase retardation between interfering arms is controlled via a phase modulator ϕ, i.e. a fiber stretcher. In our measurements, we used heralded single photons at 810 nm generated from a BBO crystal via spontaneous parametric down conversion process.

3. Results

After its first pass through the 50:50 beam splitter (BS), the single-photon wavefunction takes the form of a double-path superposition ($|\psi_{\text{in}}\rangle_\phi \sim |1\rangle_a|0\rangle_b + e^{i\phi}\ |0\rangle_a|1\rangle_b$) because the photon spatial mode occupies both arms simultaneously. Then the photon impinges on the metadevice, which is designed to have different optical response to the wavefunctions of opposite superposition states: It is completely opaque for a wavefunction which is symmetric in Fock basis ($|\psi^{(\text{S})}\rangle \sim (|1\rangle_a|0\rangle_b + |0\rangle_a|1\rangle_b)/\sqrt{2}$), whereas it is transparent for an anti-symmetric wavefunction ($|\psi^{(\text{A})}\rangle \sim (|1\rangle_a|0\rangle_b - |0\rangle_a|1\rangle_b)/\sqrt{2}$). Therefore, $|\psi_{\text{in}}\rangle_\phi$ will be modified by the metadevice in such a way that only $|\psi^{(\text{A})}\rangle$ part will be transmitted and $|\psi^{(\text{S})}\rangle$ part will be filtered out via dissipation of the photon energy to the plasmon mode, and the output state will collapses to $|\psi_{\text{out}}\rangle \sim |1\rangle_c|0\rangle_d - |0\rangle_c|1\rangle_d$.

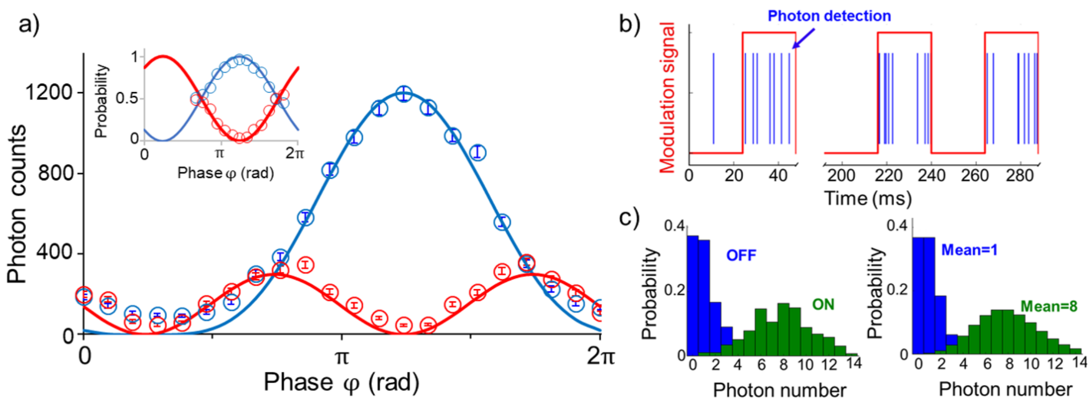

FIGURE 2: (a) Experimental results showing quantum state filtering. Error bars show the standard deviation of photon shot noise, while their sizes are typically smaller than the symbol size. Inset shows the normalized photon detection probabilities for the corresponding output arms. (b) Demonstration of all-optical control over single-photon absorption probability, where the metadevice is switched between coherent absorption (OFF) and transmission regimes (ON) with a modulation signal (shown in red). Each blue line indicates a heralded photon detection event. (c) (left) Distribution of photon counts measured at these two regimes with (right) corresponding Poisson distribution for the same mean photon number.

The experimental results agree well with the expected photon detection probabilities at two output arms of the interferometer [Fig. 2(a)]. At one output arm (i.e. blue curve), the photon detection probability changes with $(1-\sin(\phi))^2\,/\,4$, whereas it changes with $(1+\cos(2\phi))\,/\,8$ at the other arm (i.e. red curve) due to the double phase ϕ accumulation. Moreover, the phase ϕ between interfering arms also controls the probability amplitudes of the symmetric and anti-symmetric parts of the input wavefunction ($|\psi_{\text{in}}\rangle_\phi \sim (1+e^{i\phi})\ |\psi\rangle^{(S)} + (1-e^{i\phi})(|\psi\rangle^{(A)}$). Thus, phase modulation provides a way of controlling the probability of a single photon to pass through the metadevice. For a proof-of-concept experiment, we drive the metadevice between coherent absorption and transmission regimes and change the number of detected photons between a mean values of 1 and 8, respectively [Fig. 2(b)]. The distribution of photon counts detected for these regimes [Fig. 2(c) left] agrees well with the Poisson statistics of incoming photons for the same mean photon number [Fig. 2(c) right]. The non-zero photon number at the coherent absorption regimes is due to the fabrication imperfections of the fiber-metadevice.

Our work may be utilized in optical quantum information protocols such as dual rail encoding. As future work, we further investigate other metamaterial designs for processing of other forms of quantum light and study waveguide-based metadevices for scalable implementations.

References

1. T. Roger, S. Vezzoli, E. Bolduc, J. Valente, J. J. F. Heitz, J. Jeffers, C. Soci, J. Leach, C. Couteau, N. I. Zheludev, and D. Faccio, “Coherent perfect absorption in deeply subwavelength films in the single-photon regime,” Nature Communications **6** (2015).
2. C. Altuzarra, S. Vezzoli, J. Valente, W. Gao, C. Soci, D. Faccio, and C. Couteau, “Coherent perfect absorption in metamaterials with entangled photons,” ACS Photonics **4**, 2124–2128 (2017).